Low-Temperature Thermochromism Marks a Change in Coordination for the Metal Ion in Manganese Superoxide Dismutase†

Mei M. Whittaker and James W. Whittaker*

Department of Chemistry, Carnegie Mellon University, 4400 Fifth Avenue, Pittsburgh, Pennsylvania 15213

Received January 16, 1996; Revised Manuscript Received March 29, 1996⊗

ABSTRACT: We have observed thermochromism (temperature-dependent absorption) for anion complexes of manganese superoxide dismutase indicating a change in coordination number for the metal complex at low temperatures. The ligand field spectra for the Mn(III) ion, characteristic of five-coordination for the azide complex at 295 K, cleanly convert to spectra reflecting six-coordination at low temperature, with a midpoint for the transition near 200 K. *The active site structure is temperature-dependent*, a relatively rigid, distorted octahedral low-temperature Mn complex melting with dehydration (or displacement of one of the protein ligands) to form a five-coordinated complex under physiological conditions. Thermodynamic parameters for the transition estimated from van't Hoff analysis ($\Delta H_{vH} = 5$ kcal/mol; $\Delta S_{vH} = 22$ cal/mol K) are consistent with reduced chemical binding and increased fluxionality at room temperature. This thermochromism of MnSD demonstrates the existence of distinct isomeric forms of the active site metal complex, whose relative stability depends on the degree of vibrational excitation. The marginal destabilization of the six-coordinate anion complex under physiological conditions suggests that the enzyme may thermally control the stability of intermediates in a dissociative displacement mechanism for substrate binding and redox.

Superoxide dismutases are biological metal complexes that function as radical scavengers inside living cells, protecting macromolecular structures against oxidative damage (Keele et al., 1970; McCord et al., 1977; Fridovich, 1989). Three basic plans have been found for superoxide dismutase, based on mononuclear Mn or Fe or a dinuclear Cu/Zn active site (Fridovich, 1974, 1975). Each of these variants appears to be specialized in its intracellular localization (Keele et al., 1970; Ravindranath & Fridovich, 1975; Benov et al., 1995; McCord & Fridovich, 1969). The metal center (manganese, iron, or copper) in each of the known forms of SD[1] participates in catalysis by cyclically changing its oxidation state, storing an electron in a shuttle pathway for disproportionation of superoxide radicals (McCord et al., 1977):

$$2O_2^- + 2H^+ \rightarrow O_2 + H_2O_2 \qquad (1)$$

The substrate radicals are thought to directly coordinate to the metal center and undergo electron transfer within an inner sphere complex. Consistent with this view, *Escherichia coli* MnSD is inhibited by small anions, which bind to the metal ion forming stable complexes with $K_D = 7.2$ mM for azide and $K_{D,1} = 25$ mM and $K_{D,2} = 1.1$ M for the two-step binding of fluoride ion (Whittaker & Whittaker, 1991).

The primary structures of both Mn and Fe superoxide dismutases exhibit a high degree of sequence homology over a phylogenetic range from microorganisms to man (Steinman, 1982). Crystal structures for bacterial (*Thermus thermophilus*) (Ludwig et al., 1991; Lah et al., 1995) and human (Borgstahl et al., 1992) MnSD at atomic resolution likewise reveal extensive three-dimensional structural homology, with nearly identical coordination for the metal centers in each (Figure 1). The metal complex includes four protein ligands [three histidine imidazoles (from H28, H83 and H170) in NE2 nitrogen ligation and a *syn*-coordinated OD1 oxygen from an aspartic residue (D166) (*T. thermophilus* sequence labels)] as well as a water molecule or hydroxide ion. The five-coordinate structure of the ligand-free native enzyme has been described as having roughly trigonal bipyramidal geometry, with a solvent access channel opening from one equatorial edge of the coordination polyhedron. The structure of the azide complex of the *T. thermophilus* MnSD has also been solved by X-ray crystallography (Figure 1). Azide binds directly to the metal ion in the crystal, forming a complex that retains all four protein ligands. The persistence of electron density in the axial water site implies six-coordination for Mn in the anion complex (Ludwig et al., 1991; Lah et al., 1995). The metal ion appears to be displaced toward the exogenous ligand on forming the adduct to give a distorted octahedral geometry.

Spectroscopic studies on the Mn(III) sites in both ligand-free and ligand-bound forms of *Escherichia coli* MnSD have suggested that anion binding results in displacement of one of the ligands in the active site to retain five-coordination in the presence of anions (Whittaker & Whittaker, 1991). Room temperature ligand field spectra (absorption and CD) require that the coordination numbers for the native, azide, and fluoride complexes of *E. coli* MnSD all be the same. The lowest-energy d→d transition lies above 16 000 cm^{-1} in each of these complexes, well within the range of five-coordinate Mn(III) model compounds (Davis et al., 1968; Dingle, 1962, 1964, 1965). Low-temperature MCD spectra

† Support for this project from the National Institutes of Health (GM 42680) is gratefully acknowledged.

* Corresponding author. Tel: (412) 268-5670. FAX: (412) 268-6945. E-mail: jim@insight.chem.cmu.edu.

⊗ Abstract published in *Advance ACS Abstracts,* May 15, 1996.

[1] Abbreviations: VT, variable temperature; SD, superoxide dismutase; NIR, near-infrared; LMCT, ligand-to-metal charge transfer; EPR, electron paramagnetic resonance; CD, circular dichroism.

S0006-2960(96)00088-8 CCC: $12.00

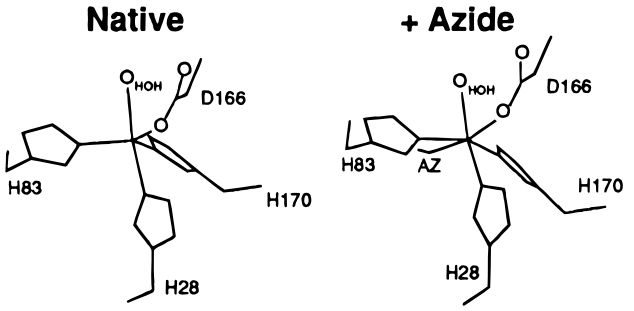

FIGURE 1: MnSD active site structure. The active site of *T. thermophilus* MnSD native enzyme (left) and azide complex (right) as defined by X-ray crystallography. [Based on published atomic coordinates (Lah et al., 1995)].

are characteristic of trigonal and tetragonal geometries for the native and anion complexes, respectively (Whittaker & Whittaker, 1991). The absence of MCD intensity in the lowest-energy ligand field band for tetragonal complexes makes the assignment of coordination numbers ambiguous in that case.

There is thus a fundamental difference in the structures identified by crystallographic and spectroscopic studies, the former characterizing the anion complexes as six-coordinate, while the latter indicating five-coordination is more likely. Recently, low-temperature X-ray absorption measurements on the azide adduct of the homologous FeSD have been used to support the crystallographic assignment of six-coordination for the corresponding complex of the manganese enzyme (Tierney et al., 1995), implying that the metal in MnSD *increases* coordination number when anions bind. On the basis of these results, Lah et al. (1995) have proposed a "5-6-5" mechanism for changes in coordination number during turnover.

In earlier work, the active site structures were assumed to be temperature-independent. To explore the possibility that the different conclusions reached in the spectroscopic and crystallographic experiments were the result of the different sample temperatures, we have used variable temperature (VT) absorption spectroscopy to study the anion complexes of *E. coli* MnSD. Both the azide and fluoride complexes exhibit an unexpected thermochromism in the ligand field spectra, undergoing an abrupt thermal transition near 200 K that implies a change from five- to six-coordination at low temperature. These results emphasize the importance of variable temperature measurements in structural biology.

MATERIALS AND METHODS

Protein. MnSD was isolated from an *E. coli* strain (AB 2463/pDT1-5) containing the *sodA* structural gene on an antibiotic resistance plasmid (Touati, 1983). This construct, which allows for high level expression of MnSD, was generously provided by Dr. Daniéle Touati of the Insitut Jacque Monod, Centre National de la Récherche Scientifique, Université Paris VII. *E. coli* AB 2463/pDT-1-5 was grown at 37 °C in 200 L of well-aerated 2× Luria−Bertani (LB) medium supplemented with 1% glucose, 2 mg of $MnSO_4 \cdot H_2O$/L, and 50 μg of ampicillin/mL. Further additions of ampicillin (100 mg/mL) were made hourly after the optical density of the culture medium reached 0.3. MnSD was purified by a modification of published procedures (Keele et al., 1979) as previously described (Whittaker & Whittaker, 1991). Superoxide dismutase activity was measured using the xanthine oxidase/cytochrome *c* inhibition assay (McCord & Fridovich, 1969). Protein concentration was determined by optical absorption measurements, using the previously reported molar extinction coefficient ($\epsilon_{280} = 8.66 \times 10^4$ M^{-1} cm^{-1}) (Beyer et al., 1989). Metal content of the purified protein was determined by atomic absorption spectrometry. The enzyme as isolated exhibits redox heterogeneity and is converted to a homogeneous Mn(III) form by molybdicyanide oxidation (Whittaker & Whittaker, 1991).

Reagents. All reagents for preparation of culture media and buffers were from commercial sources and were used without purification. Ampicillin was obtained from Sigma Chemical Co. Potassium octacyanomolybdate(IV) (molybdocyanide) was synthesized according to published procedures (Furman & Miller, 1950), and potassium molybdicyanide was prepared from the latter by permanganate oxidation (Kolthoff & Tomsicek, 1936). Solutions of potassium molybdicyanide oxidant were standardized by titration with ascorbic acid solution and analyzed for Mo by atomic absorption spectrometry.

Spectroscopic and Analytical Instrumentation. Optical absorption spectra were recorded on a Varian Instruments Cary 5E UV−vis−NIR absorption spectrometer interfaced with a microcomputer for data acquisition. To avoid condensation artifacts in the NIR, the sample chamber was purged with dry nitrogen gas. Variable temperature measurements were made using a Cryo Industries model RC-152 VT (5−300 K) vapor immersion optical cryostat, with a dual sample holder. Temperature at the sample was measured using a calibrated silicon diode sensor and a Lakeshores Cryotronics model 330 temperature controller. Samples were prepared in 50% (v/v) glycerol glassing solvent and injected into a cell formed from a pair of quartz disks separated by a silicone rubber spacer with a circular bore holding 120 μL of solution (Whittaker & Whittaker, 1991). Samples for NIR absorption measurements were prepared by exchanging protein into deuterium oxide (99.9 atom% ^2H) solvent by successive dilution and concentration cycles (to >99% exchange based on volume ratios) and mixing with glycer(ol-d_3) (98 atom% ^2H) to make a 50% (v/v) final solvent composition. Samples were cooled (<1 K/min) in a stream of helium gas at atmospheric pressure, and absorption measurements were referenced to a solvent blank prepared in parallel with the protein sample and mounted in tandem on the sample block. CD spectra were recorded on an AVIV Associates model 41DS UV−vis−NIR spectrometer as previously described (Whittaker & Whittaker, 1991), using an Air Products Heli-Tran cold finger optical cryostat and temperature controller. Glassy samples were checked for depolarization using 0.12 M nickel tartarate standard placed before and after the sample (Browett et al., 1983). Gaussian deconvolution of spectra in the energy domain was performed using the Grams/386 (Galactic Industries, Salem, NH) spectral analysis program on data truncated beyond 25 000 cm^{-1}.

RESULTS

Room temperature (295 K) optical absorption spectra for Mn(III) SD and its anion [azide(N_3^-), fluoride (F^-)] complexes are shown in Figure 2. The ligand-free and ligand-bound spectra are clearly distinct, with absorption maxima shifted to higher energy in the anion adducts [$\lambda_{max} = 449$

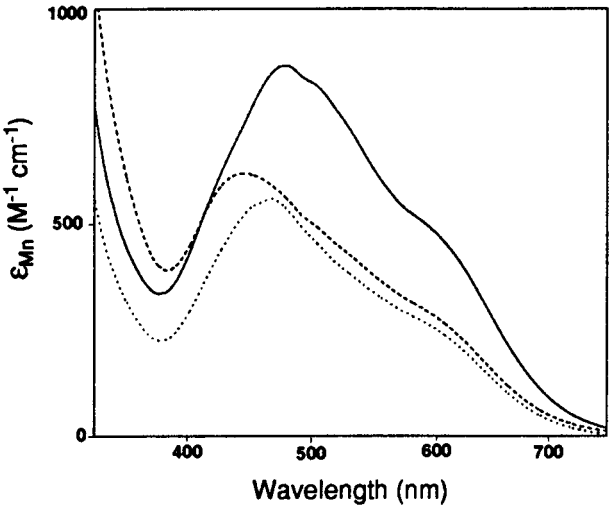

FIGURE 2: Optical absorption spectra of MnSD complexes. (—) Native MnSD (2 mM active sites in KPO_4 buffer, pH 7); (- - -) azide complex (80 mM KN_3 in KPO_4 buffer, pH 7); (···) fluoride complex (200 mM KF in KPO_4 buffer, pH 7); $T = 300$ K.

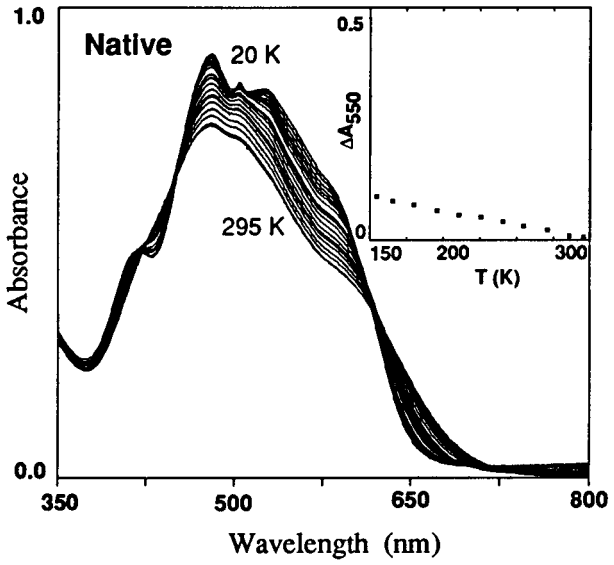

FIGURE 3: Temperature dependence of spectra for native MnSD. Experimental conditions: 5.75 mM Mn(III) SD in 50% (v/v) D_2O:glycer(ol-d_3) glassing solvent and 25 mM KPO_4 buffer, in a 2.64 mm path length cell. Temperature range for spectra: 20−295 K. The *insert* traces the thermal profile for absorption at 550 nm.

nm (N_3^-); $\lambda_{max} = 461$ nm (F^-)] relative to the native enzyme ($\lambda_{max} = 478$ nm). The lowest-energy transition in each of the complexes is below 650 nm, although weak absorption can be detected in the NIR near 1000 nm for the fluoride adduct. These spectra arise from ligand field (d→d) transitions in the metal complex (Ballhausen, 1962; Griffith, 1964) and reflect coordination number and geometry.

Temperature Dependence of the Optical Spectra (Thermochromism). The optical spectra of the Mn(III) protein gradually change at low temperature. Slow cooling of the samples in a vapor immersion cryostat permits detailed measurements of these absorption changes over a wide temperature range (20−300 K) (Figures 3 and 4). The spectrum of the ligand-free native enzyme sharpens to lower temperature, and the integrated intensity increases approximately 10%. The absorption changes are uniform over the entire temperature range, as illustrated by the insert in Figure 3, showing the thermal profile at 550 nm. The experimental data obtained over a wide range of temperatures

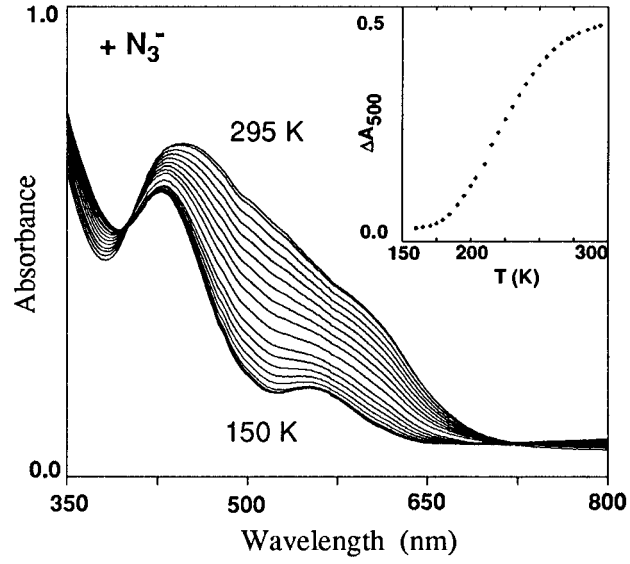

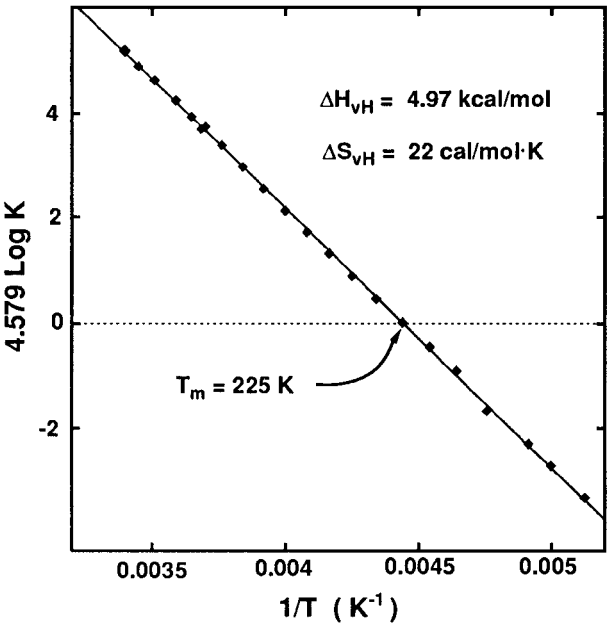

FIGURE 4: Temperature dependence of spectra for MnSD azide complex. (Above) Experimental conditions: 5.5 mM Mn(III) SD in 50% (v/v) D_2O:glycer(ol-d_3) glassing solvent containing 80 mM KN_3 and 25 mM KPO_4 buffer, in a 2.64 mm path length cell. Temperature range for spectra: 150−295 K. The *insert* traces the thermal profile for absorption at 500 nm. (Below) van't Hoff plot of thermochromic intensities for MnSD azide complex. Absorbance (A_{500}) recorded for variable temperature spectra of the MnSD azide adduct and the regression estimates of the van't Hoff heat, entropy, and compensation temperature are indicated.

(from near-ambient to cryogenic) reflect a linear decrease in absorbance as the temperature is raised:

$$A(T) = A(0)(1 + \alpha T) \qquad (2)$$

where $A(T)$ is the absorbance at temperature T, and α is the linear temperature coefficient. The magnitude of the coefficient has been determined by regression analysis of the absorption data (-9.6×10^{-4} K^{-1}).

Dramatic changes occur in the VT spectra of the azide complex, with an overall *decrease* in integrated intensity in the visible region of up to 50% at low temperature [Figure 4; similar results (not shown) are obtained for the fluoride adduct]. In contrast to the gradual and uniform changes

observed for the native enzyme spectra, there is an abrupt change in the spectra of the anion complexes, completed over a relatively narrow temperature range (approximately 100 K). Below the transition, the absorbance rises again as the temperature is further lowered, but with a small thermal coefficient similar in magnitude and sign to that observed for the native enzyme ($\alpha = -1.9 \times 10^{-3}$ K^{-1}). Isosbestics are maintained in the spectra at 415 and 730 nm (N_3^-) and at 400 and 680 nm (F^-) throughout the transition, which occurs at similar temperatures (near 210 K) for both complexes. The appearance of a broad, NIR absorption band for the anion complexes (but *not* for the ligand-free enzyme) at low temperature is perhaps the most striking feature of these spectra. This new absorption band occurs at low energy, beyond 900 nm in the near-IR, well below the lowest excitation energy observed for the 295 K spectra.

The visible−NIR CD spectra of the Mn(III) enzyme complexes complement the absorption data, resolving overlapping transitions revealing intrinsic polarization of ligand field bands arising from chirality imposed on the metal center by the protein (Charney, 1985). No significant changes occur in the CD spectra of native MnSD in the ligand field region (350−1450 nm) between 295 and 77 K other than a sharpening of spectral features at low temperature and a slight increase in intensity (Figure 5) corresponding to similar changes in the absorption spectra. On the other hand, spectra of the azide (Figure 6) and fluoride (Figure 7) complexes at ambient and low temperatures are distinct, the lowest-energy (NIR) ligand field band lacking any significant CD polarization in the liquid nitrogen temperature spectrum. These changes in the spectroscopic splittings, intensity and polarization in the ligand field spectra are consistent with a change in geometry for the Mn(III) ion, implying that *two distinct structures* are possible for the active site in the presence of anions, one structure being stable at low temperatures and the other being stable at high temperatures. These structures can in principle be defined by the ligand field spectra the Mn(III) in the protein (see Discussion, below).

Gaussian deconvolution of the broad and overlapping spectra (Figures 5−7) of the metal centers resolves individual ligand field bands and provides detailed information on the complex spectra. For a d^4 Mn(III) ion, a maximum of four spin-allowed d→d transitions are predicted for the low-symmetry split ^{5}D ground state of the free metal ion (Ballhausen, 1962), and four Gaussian components are used in fitting the visible spectra for each of the complexes. The results are listed in Table 1, which gives both energies and widths (full-width at half-maximum) for the resolved components. In each case, the absorption components correlate with features in the CD spectra recorded at the same temperature (see below). The sum of four Gaussian bands successfully reproduces each of the spectra in Figures 5−7.

Analysis. Thermochemical Parameters. The thermal transition associated with the spectral changes for the anion complexes of Mn(III) SD is reversed on warming and appears to reflect an internal structural equilibrium in the active site metal complex between high (H) and low (L) temperature isomeric forms:

$$\mathrm{L} \overset{K}{\rightleftarrows} \mathrm{H} \tag{3}$$

The distribution between these forms is defined by the equilibrium constant $K = f/(1 - f)$, f being the fraction of

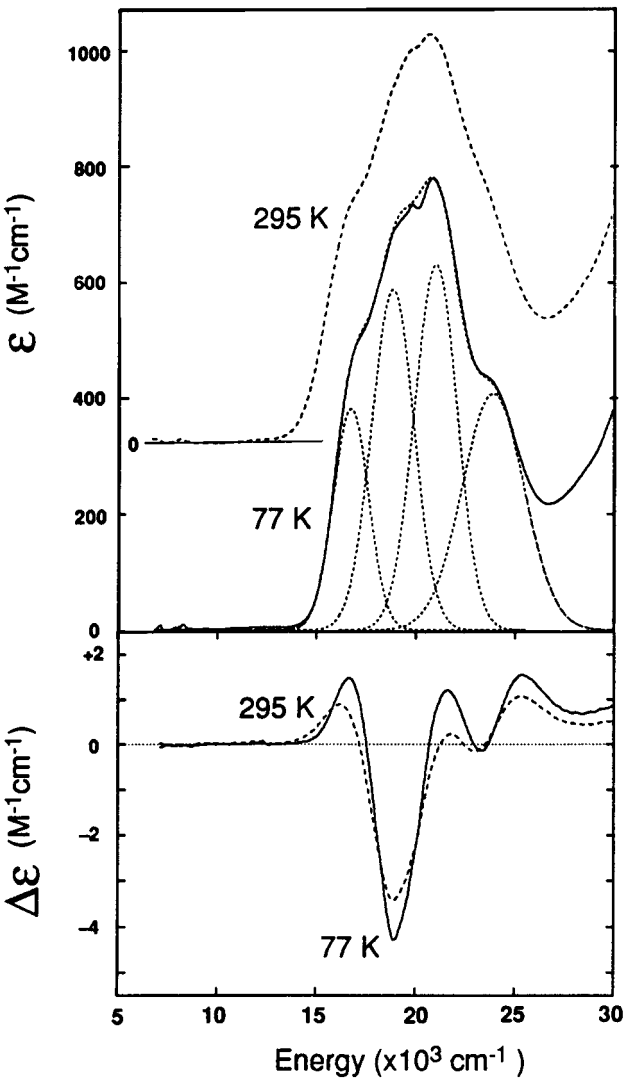

FIGURE 5: Deconvolution of ligand field spectra for native MnSD. Absorption (top) and CD (bottom) spectra at 77 K (—) and 295 K (- - -) for native MnSD prepared as described in the legend to Figure 3. The Gaussian components and their sum are superimposed on the low-temperature absorption spectrum.

limiting high-temperature form present at a given temperature. The total absorption A at a given wavelength is then the sum of weighted fractional contributions

$$A = (1 - f)A_\mathrm{L} + (f)A_\mathrm{H} \tag{4}$$

allowing the equilibrium constant to be written in terms of absorbance:

$$K = (A - A_\mathrm{L})/(A_\mathrm{H} - A) \tag{5}$$

with the limiting absorbance values (A_L and A_H) being determined by least-squares analysis of the transition data at a given wavelength. Application of the van't Hoff equation (Lewis & Randall, 1923) for the temperature dependence of the equilibrium constant

$$-\ln K = \frac{\Delta H}{RT} - \frac{\Delta S}{R} \tag{6}$$

yields the van't Hoff enthalpy and entropy (ΔH_vH and ΔS_vH) for the transition. For the azide and fluoride complexes, $\Delta H_\mathrm{vH} = 5$ kcal/mol and $\Delta S_\mathrm{vH} = 22$ cal/mol K (azide) and $\Delta H_\mathrm{vH} = 4.7$ kcal/mol and $\Delta S_\mathrm{vH} = 22$ cal/mol K

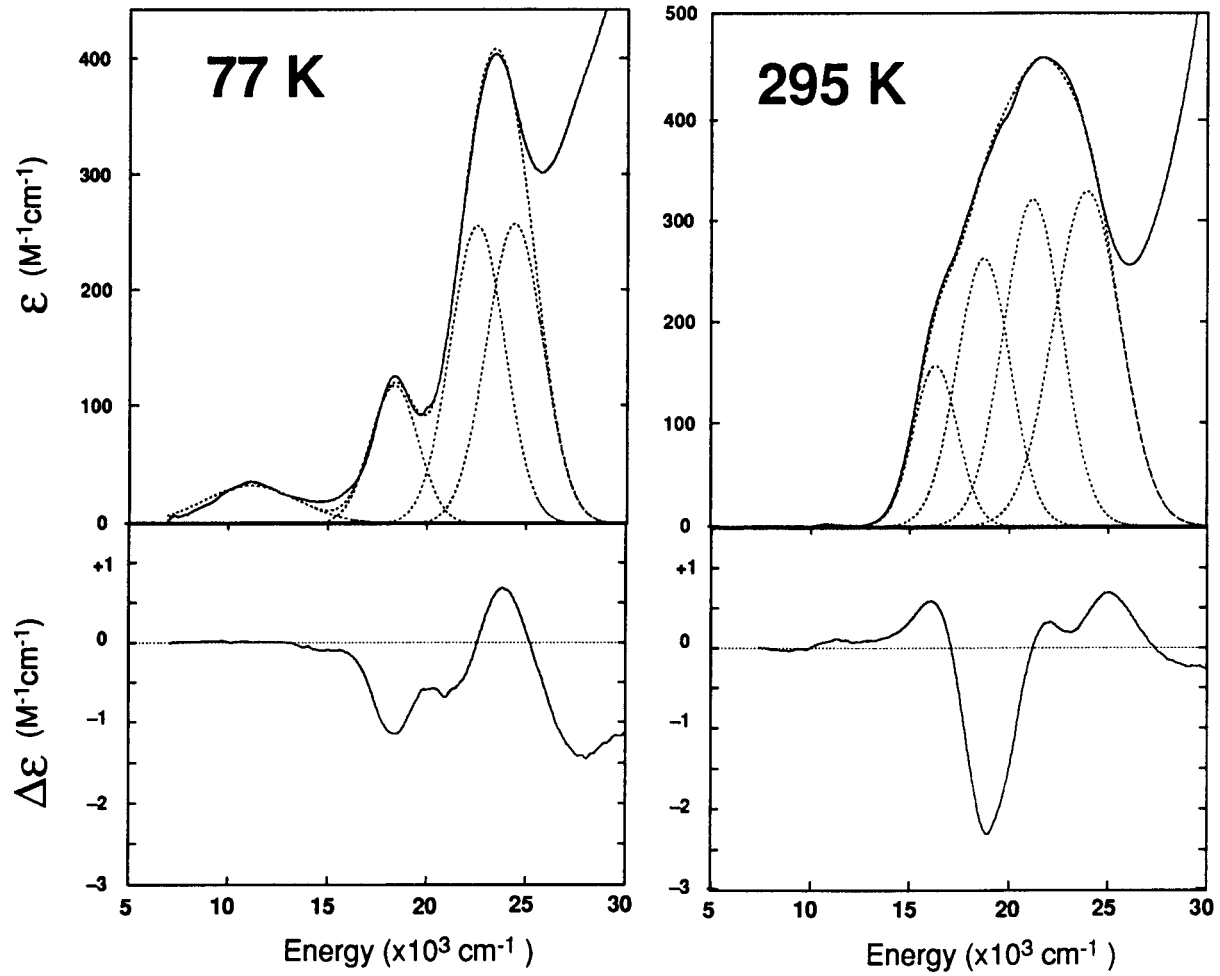

FIGURE 6: Deconvolution of ligand field spectra for MnSD azide complex. (Right) Absorption (top) and CD (bottom) spectra at 295 K for MnSD azide complex prepared as described in the legend to Figure 4. (Left) Absorption (top) and CD (bottom) spectra at 77 K for MnSD azide complex. The Gaussian components and their sum are superimposed on the absorption spectrum.

(fluoride). The midpoint of the transition (zero-crossing of the van't Hoff plot) is found to be $T_m = 225$ and 208 K for the azide and fluoride complexes, respectively. The validity of the two-state model on which this analysis is based is supported by the presence of isosbestic points between the spectra of the anion complexes that are maintained across the transition region.

DISCUSSION

Enzyme active sites are mobile structures that carry molecules through bond-making, bond-breaking, and redox processes using *dynamical motifs* that have evolved for specific aspects of catalytic function, based on the *structural motifs* that have been identified by protein crystallography (Branden & Tooze, 1991). The kinetic character of these complexes is easily overlooked in studies that lead to a static picture of enzyme structure. Variable temperature studies of structure, function, and spectra can reveal some of the dynamical aspects of the biological active site (Hopfield, 1987; Fraunfelder et al., 1991). VT optical spectroscopy (Chance, 1993; Austin & Erramilli, 1995) has been used to study the thermal behavior of protein complexes involved in electron transfer (Woodruff et al., 1984; Nocek et al., 1990; Gunner & Dutton, 1989) and ligand binding (Neya et al., 1985a,b; Stephanos & Addison, 1990). Metalloenzyme complexes can be particularly interesting for these studies because of the structural information contained in the ligand field spectra.

The complex dynamics of a functional metalloenzyme active site are set in motion by thermal excitations. Biological metal complexes adapted to a specific temperature range lose function if the conditions are changed, and there are now many examples of enzymes isolated from hyperthermophilic organisms whose catalytic activity decreases below the physiological temperatures (Adams, 1993). However, vibrations excited at higher temperatures are generally undesirable in spectroscopic and crystallographic studies, which take advantage of cryogenic conditions to reduce thermal averaging and improve sensitivity (Hope, 1988). In most studies, the effects of thermal perturbations are unknown, and variable temperature studies can be useful in evaluating the significance of low-temperature data.

Temperature-Dependent Optical Spectra. Since optical transition energies are large compared to thermal energies ($k_BT \approx 200$ cm^{-1} at $T = 295$ K), the effects of temperature in optical spectra are quite different than in low-frequency (e.g., NMR or EPR) spectroscopy. The most important thermal effects in optical spectra arise from vibronic coupling, changing covalency of metal−ligand interactions, and thermochromism relating to temperature-dependent changes in molecular structure.

Vibronic coupling mixes electronic and nuclear coordinates through the dependence of electronic energies on bond

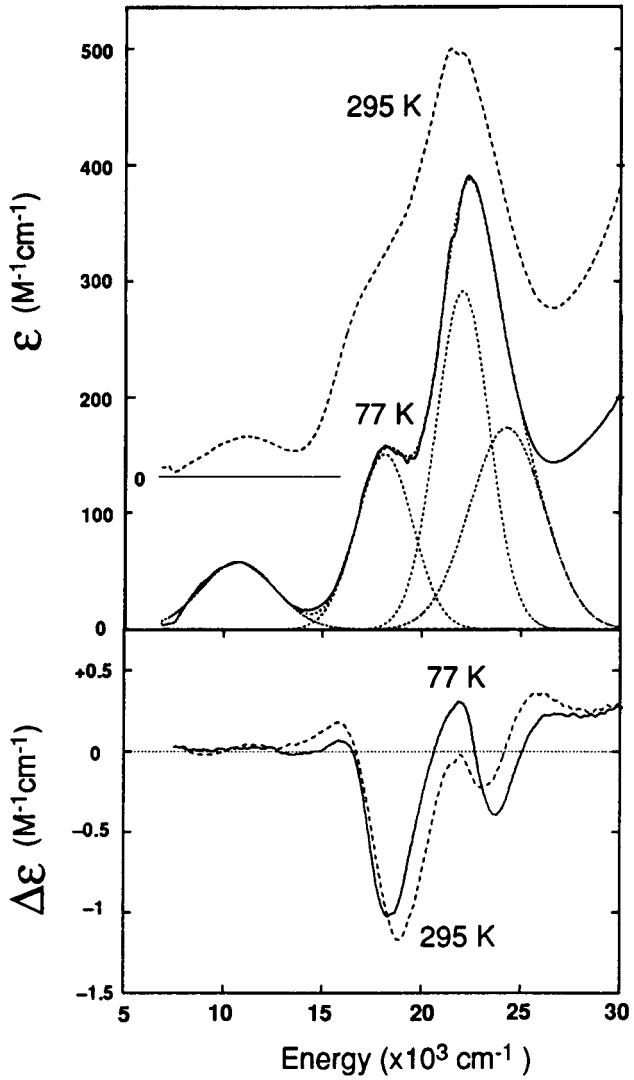

FIGURE 7: Deconvolution of ligand field spectra for MnSD fluoride complex. Absorption (top) and CD (bottom) spectra at 77 K (—) and 295 K (- - -) for MnSD fluoride complex. Experimental conditions: 5.5 mM Mn(III)SD in 50% (v/v) D_2O:glycer(ol-d_3) glassing solvent containing 200 mM KF and 25 mM KPO_4 buffer, 2.64 mm path length cell. The Gaussian components and their sum are superimposed on the low-temperature absorption spectrum.

Table 1: Spectral Components for MnSD Complexes

	77 K		295 K	
	energy (cm^{-1})	Γ (cm^{-1})[a]	energy (cm^{-1})	Γ (cm^{-1})[a]
Native				
1	16 800	2 500	16 720	3 250
2	18 900	3 000	19 025	3 060
3	21 060	3 025	21 040	3 410
4	23 950	4 400	23 700	4 740
Azide				
1	11 100	6 750	16 540	3 070
2	18 300	3 400	19 000	4 000
3	22 500	3 850	21 500	4 000
4	24 400	4 000	24 200	4 700
Fluoride				
1	10 770	5 300	11 200	5 650
2	18 150	4 000		
3	22 100	3 800		
4	24 300	5 300		

[a] Full-width at half maximum.

lengths and bond angles (Bersuker, 1975, 1984). The Jahn−Teller instability of molecules with degenerate electronic ground states [e.g., the ^5E ground state for a Mn(III) ion in O_h symmetry] is a structural consequence of vibronic coupling with a degenerate vibrational mode (Q_θ,Q_ϵ) and is expressed in the distorted structures typical of six-coordinate Mn(III) ML_6 complexes (Bersuker, 1984). Vibronic coupling can also provide a mechanism for intensity in electronically forbidden spectra (Flint, 1974) that is revealed by a characteristic temperature-dependence, the spectra growing in strength as the allowing mode is thermally excited according to a hyperbolic cotangent rule:

$$I(T) = I(0)\coth(h\nu/2k_BT) \qquad (7)$$

where $I(T)$ is the intensity at temperature T, $h\nu$ is the vibrational excitation energy for the active mode, and k_B is the Boltzmann constant (Ballhausen, 1979). Vibronic effects appear to be relatively unimportant for the Mn(III) center in SD compared to low-symmetry static distortions that lift the electronic degeneracies. The temperature coefficient for absorbance has the wrong sign to be of vibronic origin, and crystallographic data for the *T. thermophilus* MnSD azide complex reveal a large *angular* distortion from octahedral geometry, with two of the histidine ligands bending out of opposition, rather than the tetragonal stretch that is typical of a Jahn−Teller distortion for Mn(III). However, the bending modes of an octahedral complex (Nakamoto, 1986) cannot couple to the doubly degenerate electronic ground state in a vibronic Hamiltonian. Further, the low-symmetry splitting of approximately 10 000 cm^{-1} in the optical spectra is large compared to the expected vibronic energies, which have been determined to be approximately 2200 cm^{-1} for MnF_6 (Köhler et al., 1978).

In distorted complexes, combined low symmetry and covalency can give rise to intensity in ligand field spectra through admixture of allowed ligand-to-metal charge transfer (LMCT) character into the d→d transitions (DiBartolo, 1968). The covalency terms that contribute to this intensity mechanism are sensitive to metal−ligand bond parameters, and are empirically described by the linear coefficient of thermal expansion of bulk materials, implying a temperature dependence for the energy shifts of the form given in eq 2. This behavior originates in the increase in average bond length with increasing temperature arising from the anharmonicity of interatomic potentials. The negative linear coefficients for absorbance at the lowest temperatures found experimentally for all three complexes can be qualitatively understood in terms of this simple model.

A third source of temperature dependence in optical spectra is thermochromism due to changes in molecular structure (Sone & Fukuda, 1987). In contrast to the gradual temperature dependence associated with vibronic mixing and thermal changes in covalency parameters, thermochromic effects are relatively abrupt, occurring over a narrow temperature range determined by the degree of cooperativity. For a highly cooperative process (like the melting of a crystal) the transition is extremely sharp, while more gradual changes are typical of transformations of independent molecules. These transitions generally lead to an increase in both enthalpy and entropy, resulting from a decrease in chemical binding and relaxation of dynamical constraints in the higher temperature state. Inorganic thermochromism has been widely studied in nickel coordination complexes that undergo solvation/desolvation transition in solution (Mochi-

zuki et al., 1980; Sone & Fukuda, 1987). Loss of coordinated solvent at higher temperature is associated with a change in coordination number and spin state that results in dramatic changes in the optical spectra as these complexes convert between low- and high-temperature forms. Bioinorganic complexes may also exhibit thermochromism, heme proteins providing the most extensively studied examples (Neya et al., 1985a,b; Stephanos & Addison, 1990). Detailed optical studies on the spectra of small molecule complexes of several heme proteins (hemoglobin, myoglobin, and cytochrome *c*) have been used to characterize spin state and conformational equilibria for those complexes (Stephanos & Addison, 1990). However, the complexity of electronic spectra for metalloporphyrins limits the extent to which these observations can be interpreted in detailed structural terms. The copper metalloenzyme galactose oxidase has been reported to undergo a thermochromic transition associated with internal proton transfer (Whittaker & Whittaker, 1993).

Thermochemical Parameters. van't Hoff analysis of the VT spectra of the azide and fluoride complexes of MnSD yield estimates of the heats and entropies for the thermal isomerization of the active site (as described above). The magnitude of ΔH_{vH} is in the range of bond enthalpies reported for Mn(III) complexes, consistent with displacement of a ligand from the anion complexes at higher temperatures. The increase in entropy can be understood in terms of additional freedom experienced by the displaced ligand and the increased flexibility of a five-coordinate metal complex resulting from the softening of potentials for angular distortion (Kepert, 1987). Five-coordination is quite common among biological catalytic metal centers, and it is possible that the fluxionality of five-coordinate complexes (Berry, 1960; Muertterties & Guggenberger, 1974) is responsible for the selection of these complexes for catalysis.

Lumry (Lumry et al., 1966; Lumry & Biltonen, 1966) has noted that a balance between entropy and enthalpy terms in many biological processes allows transitions between structures to occur under nearly isoenergic conditions ($\Delta G = 0$) at the compensation temperature T_c ($= \Delta H/\Delta S$) corresponding to the zero-crossing point on the van't Hoff plot (Figure 4, below), the midpoint of the transition. Studies of heme proteins appear to support this picture, showing that complexes having thermal changes relating to their biological function typically exhibit compensation temperatures near ambient, while changes that are unrelated to biological function tend to have T_c remote from this condition. The T_c's determined for the azide (225 K) and fluoride (208 K) complexes of MnSD are well below ambient temperature, indicating that the active site may specifically select the higher temperature form by controlling the enthalpy and entropy content of the two complexes. At 295 K essentially complete conversion has occurred ($f > 0.90$). However, the fact that the transition has just reached completion at that point suggests that the active site is subtly poised, making the high-temperature isomeric form of the anion complex only marginally stable at 295 K. While neither azide nor fluoride is involved in normal enzyme function, their complexes can be expected to give insight into the functional interactions of the Mn(III) metal center with superoxide and peroxide anions. In particular, azide interactions will provide an effective electronic structural analog of the peroxide interactions in the product complex. Spectra of the low-temperature trapped anion complexes of *E. coli* MnSD show

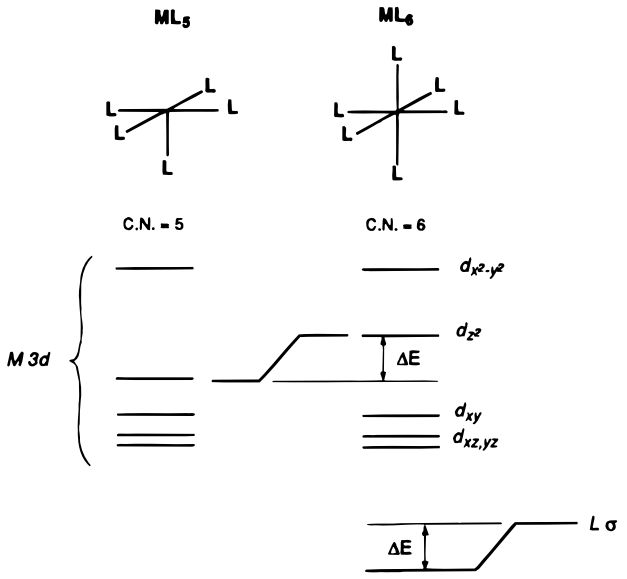

FIGURE 8: Ligand field energy diagram for five- and six-coordinate metal centers.

an uncanny similarity to spectra reported for "low-temperature" (2−6 °C) trapped complex of *T. thermophilus* MnSD with superoxide, stabilized in transient kinetics studies (Bull et al., 1991). This complex, characterized as a catalytically inactive modification that accumulates during turnover, appears to represent a six-coordinate Mn(III) center whose ligation state correlates with loss of function. The adaptation of the MnSD active site to distinct biological environments may be reflected in shifts in T_c, and studies are underway to determine the T_c for MnSD isolated from a thermophilic (high-temperature) microorganism, which may be higher than that found for the *E. coli* (mesophilic, moderate-temperature) enzyme.

Ligand Field Spectra. The ligand field spectra contain information on the structure of the thermochromic complex. High-temperature spectra of the native and azide complexes of MnSD lack significant absorption below 14 300 cm^{-1}, empirically correlating with five-coordination for Mn(III) (Davis et al., 1968; Dingle, 1962, 1965, 1966). Inspection of the crystal structure for the *T. thermophilus* MnSD (Lah et al., 1995) shows that a five-coordinate anion-bound complex cannot retain the trigonal bipyramidal geometry of the Mn(III) ion in the native enzyme and would be better described as a square pyramid. The one-electron orbital splitting diagram for a square pyramidal five-coordinate ML_5 metal complex is given in Figure 8 (left). The single ligand interaction along the *z*-axis of the complex stabilizes the (antibonding) d_{z^2} orbital relative to the corresponding level in a six-coordinate, roughly octahedral ML_6 complex (Figure 8, right). The lowest-energy transition (formally $d_{x^2-y^2} \rightarrow d_{z^2}$ in hole notation) will always lie at higher energy for complexes with five ligands than for the six-coordinated structure. From this ligand field model, the appearance of a NIR absorption band at low temperature implies conversion to a six-coordinate form. However, in exact octahedral symmetry the d_{z^2} and $d_{x^2-y^2}$ orbitals are degenerate, so the 10 000 cm^{-1} splitting measured in the optical spectrum is evidence for lower symmetry distortion. CD selection rules require both electric and magnetic dipole character in a transition (Charney, 1985). The absence of magnetic dipole character in a pure $d_{x^2-y^2} \rightarrow d_{z^2}$ transition leads to vanishing

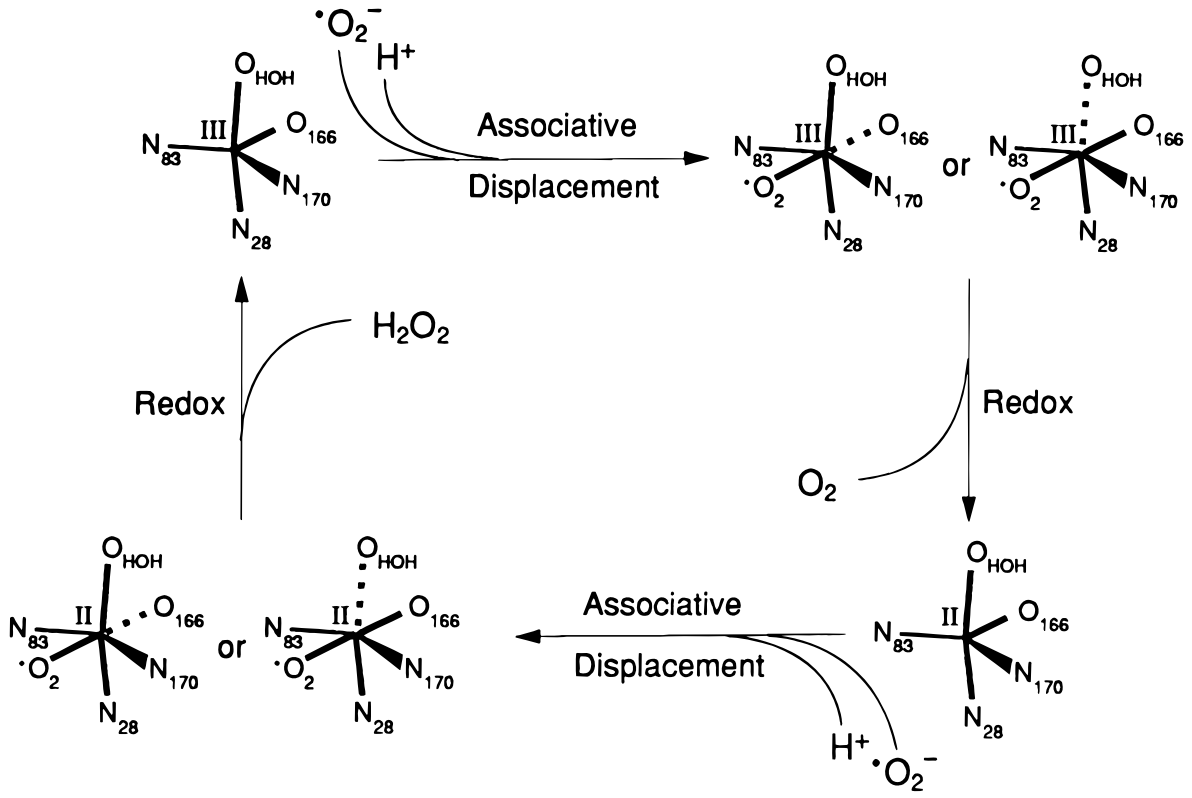

FIGURE 9: Reaction mechanism for manganese superoxide dismutase. Turnover cycle based on the associative displacement anion binding chemistry defined by variable temperature spectroscopy. Sequence numbering for the ligands is based on the *T. thermophilus* structure (Lah et al., 1995).

CD intensity for the lowest-energy Mn(III) ligand field band in an approximately tetragonal complex, which is overcome in lower symmetry by admixture of d_{xy} character into d_{z^2}. The observed changes in CD for the lowest-energy ligand field band are therefore consistent with a strong tetragonal perturbation in the low-temperature form. The red shift of the lowest-energy spin-allowed ligand field band for Mn(III) in the anion complex reflects an antibonding destabilization (ΔE) of 5440 cm^{-1} of a metal orbital corresponding to *stabilization* of a bonding orbital (of mainly ligand character) by an equivalent amount. In a crude way this gives the magnitude of the chemical binding energy for the ligand interaction. Converting units, the spectral shift leads to an estimate for the M−L bond enthalpy of 15 kcal/mol, similar to the van't Hoff heat (ΔH_{vH}) determined for the thermochromic transition (5 kcal/mol), supporting the picture of ligand displacement outlined above for this transition.

Biological Relevance. The temperature-dependent optical spectra for anion complexes of Mn(III) SD reveal a new and unexpected feature of active site chemistry, an isomerization of the structure that occurs through a thermal transition just below the physiological temperature for this enzyme. The Mn(III) ligand field spectra indicate that at 295 K, both the native and azide complexes are five-coordinate, indicating that addition of the anion must be associated with loss of one of the other ligands. There is no direct spectroscopic evidence for the identity of the ligand displaced in the anion complex, although the persistence of the near-UV azide-to-Mn(III) LMCT absorption in the 295 K spectrum indicates that the exogenous ligand remains bound. The most likely candidates for displacement on the basis of coordination chemistry and the crystallographic results are the water ligand and the carboxylate group. The Mn−OD1 (D166) carboxylate bond distance increases by 0.4 Å (to 2.25 Å) when azide is bound to *T. thermophilus* MnSD, the largest bond shift of any of the endogenous ligands (Lah et al., 1995). Carboxylate displacement would lead to an anion complex that could be described as a square-based pyramid with the exogenous ligand in the axial position. Alternatively, water may be lost through dehydration of the anion complex at elevated temperatures. Loss of coordinated solvent can occur for metal complexes that are stable in a lower coordination number and becomes more favorable as the number of anionic ligands is increased (Baes & Messmer, 1986). Dehydration would convert the complex to a square pyramid with exogenous ligand bound equatorially and histidine (H28) in the axial position. Either of these changes would be consistent with the results of our study, and the retention of the displaced ligand as a satellite in the outer sphere of the metal complex would account for the crystallographic detection of six atoms around the active site Mn in the azide complex (Lah et al., 1995).

MnSD is a metalloenzyme that is able to vary its coordination number in a temperature-dependent fashion, losing one of the endogenous ligands (protein or water) from the native enzyme complex when anions enter the coordination sphere. At low temperature, the active site is trapped in a distorted octahedral geometry, frozen in a dimple in the potential energy landscape. At higher temperature this structure melts as the active site expands into a broader region of the potential landscape characterized by weaker chemical binding but greater dynamical freedom. This transition may have important mechanistic implications relating to ligand interactions in the catalytic complexes of MnSD. The coordination changes that occur in the azide and fluoride complexes suggest that the active site may undergo succes-

sive associative displacement steps when the (anionic) superoxide subtrates bind to the active site metal center (Figure 9), with a mobile five-coordinate metal center being a key kinematic element of redox catalysis in this enzyme. The six-coordinate structure is only marginally unstable under physiological conditions, making it accessible as a kinetic intermediate in the turnover reaction. This type of thermal sculpturing of the reaction surface may be an important feature of enzyme catalysis. The results of this study emphasize the importance of thermal excitation in biological structure and function, and a role for VT spectral studies in exploring this thermal coordinate. As applications of VT spectroscopy are expanded it is likely that temperature-dependent active site structures, presently regarded as exceptional, will be found to be the rule in biology.

REFERENCES

Adams, M. W. W. (1993) *Annu. Rev. Microbiol. 47*, 627−658.

Austin, R. H., & Erramilli, S. (1995) *Methods Enzymol. 246*, 131−168.

Baes, C. F., Jr., & Messmer, R. E. (1986) *The Hydrolysis of Metal Cations*, R. E. Kreiger Publishing Co., Malabar, FL.

Ballhausen, C. J. (1962) *Introduction to Ligand Field Theory*, McGraw-Hill, San Francisco.

Ballhausen, C. J. (1979) *Molecular Electronic Structures of Transition Metal Complexes*, McGraw-Hill, San Francisco.

Benov, L., Chang, L. Y. Day, B., & Fridovich, I. (1995) *Arch. Biochem. Biophys. 319*, 508−511.

Berry, R. S. (1960) *Rev. Mod. Phys. 32*, 447−454.

Bersuker, I. B. (1975) *Coord. Chem. Rev. 14*, 357−412.

Bersuker, I. B. (1984) *The Jahn−Teller Effect and Vibronic Interactions in Modern Chemistry*, Plenum, New York.

Beyer, W. F., Reynolds, J. A., & Fridovich, I. (1989) *Biochemistry 28*, 4403−4409.

Borgstahl, G. E. O., Parge, H. E., Hickey, M. J., Beyer, W. F., Jr., Hallewell, R. A., & Tainer, J. A. (1992) *Cell 71*, 107−118.

Branden, C., & Tooze, J. (1991) *Introduction to Protein Structure*, Garland Publishing, New York.

Breza, M., Pelikán, P., & Boca, R. (1986) *Polyhedron 10*, 1607−1613.

Browett, W. R., Fucaloro, A. F., Morgan, T. V., & Stephens, P. J. (1983) *J. Am. Chem. Soc. 105*, 1868−1872.

Bull, C., Niederhoffer, E. C., Yoshida, T., & Fee, J. A. (1991) *J. Am. Chem. Soc. 113*, 4069−4076.

Chance, M. R. (1993) *Methods Enzymol. 226*, 97−118.

Charney, E. (1985) *The Molecular Basis of Optical Activity*, Krieger Publishing Co., Malabar, FL.

Cupane, A., Leone, M., Militello, V., Stroppolo, M. E., Polticelli, F., & Desidero, A. (1994) *Biochemistry 33*, 15103−15109.

Cupane, A., Leone, M., Militello, V., Stroppolo, M. E., Polticelli, F., & Desidero, A. (1995) *Biochemistry 34*, 16313−16319.

Davis, T. S., Fackler, J. P., & Weeks, M. J. (1968) *Inorg. Chem. 7*, 1994−2002.

Day, J. H. (1968) *Chem. Rev. 68*, 649−657.

DiBartolo, B. (1968) *Optical Interactions in Solids*, John Wiley, New York.

Dingle, R. (1962) *J. Mol. Spectrosc. 9*, 426−427.

Dingle, R. (1965) *Inorg. Chem. 4*, 1287−1290.

Dingle, R. (1966) *Acta Chem. Scand. 20*, 33−44.

Fackler, J. P., Jr., & Chawla, I. D. (1964) *Inorg. Chem. 3*, 1130−1134.

Flint, C. D. (1974) *Coord. Chem. Rev. 14*, 47−66.

Fraunfelder, H., Sligar, S. G., & Wolynes, P. G. (1991) *Science 254*, 1598−1603.

Fridovich, I. (1974) *Adv. Enzymol. 41*, 35−97.

Fridovich, I. (1975) *Annu. Rev. Biochem. 44*, 147−159.

Fridovich, I. (1989) *J. Biol. Chem. 264*, 7761−7764.

Furman, N. H., & Miller, C. O. (1950) *Inorg. Synth. 3*, 160−163.

Griffith, J. S. (1964) *Theory of Transition-Metal Ions*, Cambridge University Press, Cambridge, U.K.

Gunner, M. R., & Dutton, P. L. (1989) *J. Am. Chem. Soc. 111*, 3400−3412.

Hope, H. (1988) *Acta Crystallogr. Sect. B.: Struct. Sci. B44*, 22−26.

Hopfield, J. J. (1987) in *Protein Structure: Molecular and Electronic Reactivity* (Austin, R., Buhks, B., Chance, B., De Vault, D., Dutton, P. L., Fraunfelder, H., & Gol'danskii, V. I., Eds.) pp 167−185, Springer-Verlag, New York.

Keele, B. B., Jr., McCord, J. M., & Fridovich, I. (1970) *J. Biol. Chem. 245*, 6176−6181.

Kepert, D. L. (1987) in *Comprehensive Coordination Chemistry* (Wilkinson, G., Gillard, R. D., & McCleverty, J. A, Eds.) Vol. 1, pp 31−103, Pergamon Press, NewYork.

Köhler, P., Massa, W., Reinen, D., Hofmann, B., & Hoppe, R. (1978) *Z. Anorg. Allg. Chem. 446*, 131−158.

Kolthoff, I. M., & Tomsicek, W. J. (1936) *J. Phys. Chem. 40*, 247−255.

Lah, M. S., Dixon, M. M., Pattridge, K. A., Stallings, W. C., Fee, J. A., & Ludwig, M.L. (1995) *Biochemistry 34*, 1646−1660.

Lewis, G. N., & Randall, M. (1923) *Thermodynamics and the Free Energy of Chemical Substances*, McGraw-Hill, San Francisco.

Ludwig, M. L., Metzger, A. L., Pattridge, K. A., & Stallings, W. C. (1991) *J. Mol. Biol. 219*, 335−358.

Lumry, R., & Biltonen, R. (1969) in *Biological Macromolecules* (Timascheff, T., & Fasman, G. D., Eds.) Vol. 2, Dekker, New York.

Lumry, R., Biltonen, R., & Brandts, J. F. (1966) *Biopolymers 4*, 917−944.

McCord, J. M., & Fridovich, I. (1969) *J. Biol. Chem. 244*, 6049−6055.

McCord, J. M., Boyle, J. A., Day, E. D., Jr., Rizzolo, L. J., & Salin, M. L. (1977) in *Superoxide and Superoxide Dismutases* (Michelson, A. M., McCord, J. M., & Fridovich, I., Eds.) pp 129−138, Academic, New York, 1977.

Mochizuki, K., Masatoshi, F., Ito, H., & Ito, T. (1980) *Bull. Chem. Soc. Jpn. 53*, 2535−2539.

Muetterties, E. L. (1971) *Acc. Chem. Res. 3*, 266−273.

Muertterties, E. L., & Guggenberger, L. J. (1974) *J. Am. Chem. Soc. 96*, 1748−1756.

Nakamoto, K. (1986) *Infrared and Raman Spectra*, 4th ed., pp 147−148, J. Wiley, New York.

Neya, S., Hada, S., & Funasaki, N. (1985a) *Biochim. Biophys. Acta 827*, 241−246.

Neya, S., Hada, S., Funasaki, N., Umemura, J., & Takenaka, T. (1985b) *Biochim. Biophys. Acta 827*, 157−163.

Nocek, J. M., Liang, N., Wallin, S. A., Mauk, A. G., & Hoffman, B. M. (1990) *J. Am. Chem. Soc. 112*, 1623−1625.

Ravindranath, S. D., & Fridovich, I. (1975) *J. Biol. Chem. 250*, 6107−6112.

Sone, K., & Fukuda, Y. (1987) *Inorganic Thermochromism*, Springer Verlag, New York.

Steinman, H. M. (1982) in *Superoxide Dismutase* (Oberly, L. W., Ed.) Vol. 1, pp 11−68, CRC Press, Boca Raton, FL.

Stephanos, J. J., & Addison, A. W. (1990) *J. Inorg. Biochem. 39*, 351−369.

Tierney, D., Ludwig, M. L., Fee, J. A., & Penner-Hahn, J. E. (1995) *Biochemistry 34*, 1661−1668.

Touati, D. (1983) *J. Bacteriol. 155*, 1078−1087.

Whittaker, J. W., & Whittaker, M. M. (1991) *J. Am. Chem. Soc. 113*, 5528−5540.

Whittaker, M. M., & Whittaker, J. W. (1988) *J. Biol. Chem. 263*, 6074−6080.

Whittaker, M. M., & Whittaker, J. W. (1993) *Biophys. J. 64*, 762−772.

Woodruff, W. H., Norton, K. A., Swanson, B. I., & Fry, H. A. (1984) *Proc. Natl. Acad. Sci. U.S.A. 81*, 1263−1267.

BI960088M